The Astronomical Journal, 154:66 (14pp), 2017 August https://doi.org/10.3847/1538-3881/aa7b70

The Densities of Planets in Multiple Stellar Systems

E. Furlan[1] and S. B. Howell[2]
[1] IPAC, Mail Code 314-6, Caltech, 1200 E. California Blvd., Pasadena, CA 91125, USA; furlan@ipac.caltech.edu
[2] NASA Ames Research Center, Moffett Field, CA 94035, USA
Received 2017 April 13; revised 2017 June 19; accepted 2017 June 21; published 2017 July 24

Abstract

We analyze the effect of companion stars on the bulk density of 29 planets orbiting 15 stars in the *Kepler* field. These stars have at least one stellar companion within 2″, and the planets have measured masses and radii, allowing an estimate of their bulk density. The transit dilution by the companion star requires the planet radii to be revised upward, even if the planet orbits the primary star; as a consequence, the planetary bulk density decreases. We find that if planets orbited a faint companion star, they would be more volatile-rich, and in several cases their densities would become unrealistically low, requiring large, inflated atmospheres or unusually large mass fractions in an H/He envelope. In addition, for planets detected in radial velocity data, the primary star has to be the host. We can exclude 14 planets from orbiting the companion star; the remaining 15 planets in seven planetary systems could orbit either the primary or the secondary star, and for five of these planets the decrease in density would be substantial even if they orbited the primary, since the companion is of almost equal brightness as the primary. Substantial follow-up work is required in order to accurately determine the radii of transiting planets. Of particular interest are small, rocky planets that may be habitable; a lower mean density might imply a more volatile-rich composition. Reliable radii, masses, and thus bulk densities will allow us to identify which small planets are truly Earth-like.

Key words: binaries: general – planets and satellites: composition – planets and satellites: fundamental parameters

1. Introduction

With more than 3000 exoplanets known to date, most of them discovered by the *Kepler* mission (Borucki et al. 2010) and increasing numbers by its successor *K2* (Howell et al. 2014), it has become clear that planetary systems vary widely in their properties and that our Solar System might be in a unique configuration. Besides the number of planets around a given star and their orbital spacing, a fundamental quantity is a planet's density. The bulk density of a planet gives us clues as to its composition (e.g., Fortney et al. 2007; Seager et al. 2007; Rogers et al. 2011; Rogers 2015; Zeng et al. 2016): a higher density is indicative of a rocky interior, while a low density suggests a planet surrounded by a substantial atmosphere. Of particular interest are rocky planets with liquid water on their surface and an atmosphere, which, if at a suitable distance from their star, might be able to support life as we know it.

In order to determine a planet's mean density, its mass and radius have to be known. The *Kepler* mission discovered planets by the transit method, which measures the dimming of the stellar light as the planet passes in front of its star. The observed transit depth yields the radius of the planet, assuming that the stellar radius is known. The mass is typically determined from radial velocity (RV) follow-up measurements of the planet (e.g., Marcy et al. 2014); in some cases of multiple planetary systems, transit-timing variations (TTVs) can be used to determine planetary masses (e.g., Hadden & Lithwick 2014). Uncertainties in the determination of the planet's radius and mass propagate to uncertainties in the planet's density.

Besides the usual measurement uncertainties, one factor can affect the reliable determination of a planet's radius: the presence of one or more stellar companions. The transit method derives the planet's radius from the transit depth, which is the difference of the out-of-transit and in-transit flux relative to the out-of-transit flux. A stellar companion dilutes the transit, making it appear shallower, and thus we infer a smaller planetary radius. Therefore, the presence of close companions leads to an underestimate of planetary radii. These companions are not necessarily bound to the primary star; studies of *Kepler* stars have shown that most companions within 1″ are bound, while this applies to only ∼50% of companions at 2″ (Horch et al. 2014; Hirsch et al. 2017). However, even a close background star will dilute the transit and require a revision of the derived planet radius.

When planetary radii are underestimated, their density is overestimated, which is an issue of particular importance for small, rocky, potentially habitable planets. With a close companion star present, the radius of such a "small" planet would have to be revised upward, possibly requiring a substantial gaseous envelope to explain the resulting lower bulk density. Recently, seven Earth-sized planets were discovered transiting the nearby star TRAPPIST-1 (Gillon et al. 2016, 2017); their densities suggest a rocky composition with a certain fraction of volatiles (Gillon et al. 2017). Howell et al. (2016) carried out speckle imaging of TRAPPIST-1 and were able to exclude a companion star or brown dwarf from 0.32 to 14.5 au from the star; their results complemented the RV measurements from Barnes et al. (2014), which ruled out stellar companions within about 0.15 au. Thus, follow-up observations established that the radii of the TRAPPIST-1 planets derived from transits are correct.

For the *Kepler* mission, a substantial imaging and spectroscopic follow-up observation program was carried out (for a summary, see Furlan et al. 2017 and references therein; E. Furlan et al. 2017b, in preparation). The aim of the imaging program was to detect companion stars to planet host stars, while the main goal of the spectroscopic program was to refine stellar parameters. RV measurements (which require high spectral resolution) are mainly used to determine lanet masses, but they can also reveal close companion stars

(Kolbl et al. 2015). However, only a certain range of parameter space can be probed by spectroscopy; companions that are too faint, too far, or too similar to the primary star cannot be detected. Teske et al. (2015) showed that the RV detections can be very uncertain; beyond about 0.″02, high-resolution imaging yields more reliable and complete information on stellar companions. From the compilation of high-resolution and seeing-limited imaging of KOI host stars in Furlan et al. (2017), we find that about 6% (11%) of the detected companions lie within 0.″5 (1.″0) from their primary stars and have median Δm values of 0.9 (1.5) in the K band and 1.0 (1.3) in the i band.

From the solar neighborhood, we know that about 44% of solar-type stars have a bound companion within ~10,000 au, with most companions at separations between a few and a few hundred au (Raghavan et al. 2010). The multiplicity of stars in the *Kepler* field, which lie at distances up to a few kiloparsecs (the median distance is 840 pc; Mathur et al. 2017), has not yet been well established. Horch et al. (2014) carried out simulations of the *Kepler* field using a companion star fraction of 40%–50% and the distribution of binaries in the solar neighborhood (Duquennoy & Mayor 1991; Raghavan et al. 2010), and they were able to reproduce their observed companion star fractions from speckle observations. Their results implied that about half of *Kepler* stars have companions, even though not all of them can be detected. However, several recent studies found lower stellar multiplicity rates for host stars of KOI planets, especially at projected separations less than a few tens up to a few hundred au (Wang et al. 2014a, 2014b, 2015a, 2015b; Kraus et al. 2016). On the other hand, due to detection and sensitivity limits, some parts of the binary parameter space, e.g., companions at separations $\lesssim$10 au (accessible only via RV measurements) or companions with $\Delta m \gtrsim 3$ at $\lesssim$20 au (in high-resolution images), have not yet been fully explored.

The detectability of stellar companions depends not only on their projected separations from the primary star but also on their relative brightness. Raghavan et al. (2010) found that the mass-ratio distribution for stars in multiple systems is mostly flat, with a deficit at low values ($\lesssim$0.2) but a sharp increase in the number of companions with mass ratios close to unity. From the data presented in Raghavan et al. (2010), we deduce that the fraction of about equal mass systems (mass ratio >0.9) is 17% ± 3%; this fraction increases to 27% ± 5%, 30% ± 6%, and 38% ± 10% for stars with about equal mass companions within 100, 50, and 10 au, respectively. Thus, we can infer that about 15% of stars (at least in the solar neighborhood, perhaps also in the *Kepler* field) have such bright, close companions; it is this type of companions that have the strongest effect on derived planet radii if planets are assumed to orbit their primary star. Equal-brightness binaries increase the planet radius (derived under the assumption that the star is single) the most, namely, by a factor of 1.4. Planets that orbit a star with a fainter companion typically have radii underestimated by a few percent (Furlan et al. 2017).

A scenario rarely considered in the literature is the possibility that a planet could orbit a fainter companion star. In this case its radius would need a correction by a factor of a few (Furlan et al. 2017). It is necessary to assess each system to determine which star the planet likely orbits, but in some cases, the companion star can be excluded as being the host star based on the lack of significant centroid shifts (e.g., Latham et al. 2010; Bryson et al. 2013) or on the color of the companion star (e.g., Howell et al. 2012; Hirsch et al. 2017). In other cases, more thorough follow-up work, especially a statistical analysis of the available data, is needed to determine the actual host star and thus an accurate planet radius (e.g., Barclay et al. 2015). We note that in cases of very close stellar companions ($\lesssim$ a few au), planets might actually orbit both stars. In fact, there are planets known to orbit eclipsing binary stars in the *Kepler* field (e.g., Doyle et al. 2011; Orosz et al. 2012; Welsh et al. 2012; Schwamb et al. 2013; Kostov et al. 2016). Since the radii of eclipsing binary stars can be measured quite accurately, the radii of planets orbiting them are fairly reliable, too.

In Furlan et al. (2017), we calculated planet radius correction factors for all those *Kepler* planet host stars with a stellar companion within 4″. We assumed companion stars to be bound to the primary stars and thus at the same distance from Earth, so properties such as their stellar radius could be estimated. Our results agreed with those from Ciardi et al. (2015), who used the multiplicity fraction and mass ratio distribution from Raghavan et al. (2010) and estimated that, on average, the radii of *Kepler* planets are underestimated by a factor of 1.5.

In this work, we use the results presented in Furlan et al. (2017) and apply them to *Kepler* planets whose masses have been determined in addition to the radii derived from the transit observations. We estimate the change in radius and thus density for the planets and discuss the implications for the planets' composition. We present our sample in Section 2, our results in Section 3, and our discussion in Section 4; Section 5 contains our conclusions.

2. Sample

In Furlan et al. (2017), we combined measurements of detected companions within 4″ (one *Kepler* pixel) of host stars of *Kepler* Objects of Interest (KOIs) and created a catalog of 2297 companions around 1903 primary stars. The KOIs can be either planet candidates or false positives; only follow-up observations (RV measurements, high-resolution imaging) can confirm a planet candidate as an actual planet, but planets have also been validated by analyzing observational results with statistical methods (see, e.g., Rowe et al. 2014; Morton et al. 2016). Here we only select *Kepler* stars that are hosts to confirmed planets and have one or more companions within 2″ listed in Furlan et al. (2017). Companions at these projected separations are more likely to be bound (see Horch et al. 2014; Hirsch et al. 2017) and are also unlikely to be detected by the *Kepler* photometric centroid shift analysis (Bryson et al. 2013); also, none of these companions are listed in the *Kepler* Input Catalog (KIC). A close companion, even if unbound, will dilute the transit depth and thus affect the derived planet radius. Moreover, we limit our sample to confirmed *Kepler* planets with measured masses (including upper limits) and radii, which allows us to infer the bulk density of the planets. Additionally, we exclude those planets from further analysis for which no correction to the planet radius is needed, as detailed below.

Table 1 lists all confirmed *Kepler* planets with masses, radii, and at least one companion star within 2″ from the compilation of Furlan et al. (2017). This sample amounts to 50 planets orbiting 26 stars. We adopted planetary mass and radius measurements from the literature (as collected by the NASA Exoplanet Archive[3]). When more than one measurement was

[3] http://exoplanetarchive.ipac.caltech.edu

Table 1
Masses, Radii, and Planet Radius Correction Factors of Confirmed *Kepler* Planets Orbiting Stars with Stellar Companions at $\leqslant 2''$

Planet Name (1)	KOI (2)	KICID (3)	Mass (M_J) (4)	Radius (R_J) (5)	Mass Flag (6)	Blend Flag (7)	$PRCF_p$ (8)	$PRCF_s$ (9)	References (10)
Kepler-1 b	1	11446443	1.2232 ± 0.018	1.213 ± 0.011	R, M	1	…	…	1, 6, 8, 11, 15, 16, 24, 28, 29, 31, 32, 33
Kepler-5 b	18	8191672	2.0818 ± 0.033	1.339 ± 0.023	R, M	1	…	…	11, 19, 29
Kepler-7 b	97	5780885	0.4367 ± 0.024	1.604 ± 0.015	R, M	1	…	…	11, 17, 29, 30
Kepler-10 b	72	11904151	0.0126 ± 0.002	0.130 ± 0.001	R	0	1.000	…	2, 9, 11, 12
Kepler-10 c	72	11904151	0.0540 ± 0.006	0.210 ± 0.006	R	0	1.000	…	9
Kepler-11 b	157	6541920	0.0105 ± 0.003	0.161 ± 0.004	T	0	1.003	…	13, 20, 21
Kepler-11 c	157	6541920	0.0187 ± 0.006	0.257 ± 0.005	T	0	1.003	…	13, 20, 21
Kepler-11 d	157	6541920	0.0215 ± 0.003	0.279 ± 0.006	T	0	1.003	…	13, 20, 21
Kepler-11 e	157	6541920	0.0249 ± 0.005	0.374 ± 0.008	T	0	1.003	…	13, 20, 21
Kepler-11 f	157	6541920	0.0067 ± 0.003	0.221 ± 0.005	T	0	1.003	…	13, 20, 21
Kepler-11 g	157	6541920	<0.0790	0.297 ± 0.006	T	0	1.003	…	21
Kepler-13 b	13	9941662	9.0250 ± 0.205	1.461 ± 0.026	M	1	…	…	11, 27
Kepler-14 b	98	10264660	8.0620 ± 0.259	1.130 ± 0.040	R, M	1	…	…	5, 30
Kepler-21 b	975	3632418	0.0160 ± 0.005	0.146 ± 0.001	R	0	1.002	…	18
Kepler-27 b	841	5792202	0.1320 ± 0.018	0.522 ± 0.024	T	0	1.014	3.430	13
Kepler-27 c	841	5792202	0.0670 ± 0.011	0.640 ± 0.029	T	0	1.014	3.430	13
Kepler-53 b	829	5358241	0.3240 ± 0.106	0.253 ± 0.061	T	0	1.054	1.820	13
Kepler-53 c	829	5358241	0.1120 ± 0.053	0.278 ± 0.067	T	0	1.054	1.820	13
Kepler-64 b	6464	4862625	<0.5310	0.551 ± 0.015	R, M	1	…	…	26
Kepler-74 b	200	6046540	0.6586 ± 0.073	1.005 ± 0.025	R	0	1.032	…	3, 14
Kepler-80 b	500	4852528	0.0218 ± 0.002	0.238 ± 0.009	T	0	1.002	5.343	22
Kepler-80 c	500	4852528	0.0212 ± 0.004	0.244 ± 0.010	T	0	1.002	5.343	22
Kepler-80 d	500	4852528	0.0212 ± 0.002	0.136 ± 0.007	T	0	1.002	5.343	22
Kepler-80 e	500	4852528	0.0130 ± 0.003	0.143 ± 0.007	T	0	1.002	5.343	22
Kepler-84 b	1589	5301750	0.1260 ± 0.038	0.174 ± 0.045	T	0	1.202	1.387	13
Kepler-84 c	1589	5301750	0.0640 ± 0.037	0.184 ± 0.047	T	0	1.202	1.387	13
Kepler-92 b	285	6196457	0.2020 ± 0.044	0.313 ± 0.009	T	0	1.002	3.079	34
Kepler-92 c	285	6196457	0.0190 ± 0.006	0.232 ± 0.007	T	0	1.002	3.079	34
Kepler-97 b	292	11075737	0.0110 ± 0.006	0.132 ± 0.012	R	0	1.029	…	23
Kepler-100 b	41	6521045	0.0230 ± 0.010	0.118 ± 0.004	R	0	1.008	3.604	23
Kepler-100 c	41	6521045	<0.0222	0.196 ± 0.004	R	0	1.008	3.604	23
Kepler-100 d	41	6521045	<0.0094	0.144 ± 0.004	R	0	1.008	3.604	23
Kepler-104 b	111	6678383	0.0620 ± 0.043	0.279 ± 0.054	T	0	1.001	6.059	13
Kepler-106 b	116	8395660	<0.0167	0.073 ± 0.010	R	0	1.000	…	23
Kepler-106 c	116	8395660	0.0330 ± 0.010	0.223 ± 0.029	R	0	1.000	…	23
Kepler-106 d	116	8395660	<0.0255	0.085 ± 0.012	R	0	1.000	…	23
Kepler-106 e	116	8395660	0.0350 ± 0.018	0.228 ± 0.029	R	0	1.000	…	23
Kepler-145 b	370	8494142	0.1170 ± 0.036	0.236 ± 0.007	T	0	1.000	…	34
Kepler-145 c	370	8494142	0.2500 ± 0.052	0.385 ± 0.011	T	0	1.000	…	34
Kepler-203 c	658	6062088	2.3600 ± 1.202	0.186 ± 0.046	T	0	1.009	3.326	13
Kepler-203 d	658	6062088	0.1070 ± 0.340	0.109 ± 0.027	T	0	1.009	3.326	13
Kepler-326 b	1835	9471268	0.1400 ± 0.127	0.270 ± 0.159	T	0	1.407	1.421	13
Kepler-326 c	1835	9471268	0.0550 ± 0.041	0.249 ± 0.146	T	0	1.407	1.421	13
Kepler-326 d	1835	9471268	0.0220 ± 0.023	0.215 ± 0.126	T	0	1.407	1.421	13
Kepler-333 b	1908	5706966	0.0890 ± 0.083	0.144 ± 0.015	T	0	1.009	2.970	13
Kepler-396 b	2672	11253827	0.2380 ± 0.027	0.312 ± 0.086	T	0	1.001	2.733	34

Table 1
(Continued)

Planet Name (1)	KOI (2)	KICID (3)	Mass (M_J) (4)	Radius (R_J) (5)	Mass Flag (6)	Blend Flag (7)	$PRCF_p$ (8)	$PRCF_s$ (9)	References (10)
Kepler-396 c	2672	11253827	0.0560 ± 0.007	0.473 ± 0.131	T	0	1.001	2.733	34
Kepler-424 b	214	11046458	1.0300 ± 0.130	0.890 ± 0.070	R	0	1.001	…	10
Kepler-432 b	1299	10864656	5.2251 ± 0.232	1.132 ± 0.026	R	1	…	…	7, 25
Kepler-448 b	12	5812701	<10.0	1.430 ± 0.130	R	0	1.021	…	4

Note. Columns: (1) *Kepler* planet name; (2) KOI number of the star; (3) identifier of the star from the *Kepler* Input Catalog (KIC); (4) mass of the planet; (5) radius of the planet; (6) methods by which the mass was determined ("R"—RV; "T"—TTV; "M"—light-curve model); (7) flag to indicate whether the blending by a nearby companion was already accounted for when the planet radius was derived in at least one of the references listed in column (10) (1—yes; 0—no); (8) and (9) planet radius correction factors assuming that the planet orbits the primary or brightest secondary star, respectively, from Furlan et al. (2017); (10) references for planet mass and radius.

References. (1) Barclay et al. 2012; (2) Batalha et al. 2011; (3) Bonomo et al. 2015; (4) Bourrier et al. 2015; (5) Buchhave et al. 2011; (6) Christiansen et al. 2011; (7) Ciceri et al. 2015; (8) Daemgen et al. 2009; (9) Dumusque et al. 2014; (10) Endl et al. 2014; (11) Esteves et al. 2015; (12) Fogtmann-Schulz et al. 2014; (13) Hadden & Lithwick 2014; (14) Hébrard et al. 2013; (15) Holman et al. 2007; (16) Kipping & Bakos 2011; (17) Latham et al. 2010; (18) López-Morales et al. 2016; (19) Koch et al. 2010; (20) Lissauer et al. 2011; (21) Lissauer et al. 2013; (22) MacDonald et al. 2016; (23) Marcy et al. 2014; (24) O'Donovan et al. 2006; (25) Quinn et al. 2015; (26) Schwamb et al. 2013; (27) Shporer et al. 2014; (28) Southworth 2010; (29) Southworth 2011; (30) Southworth 2012; (31) Sozzetti et al. 2007; (32) Torres et al. 2008; (33) Turner et al. 2016; (34) Xie 2014.

available, we calculated a weighted average using the inverse of the uncertainty as weights. The column "blend flag" in Table 1 indicates whether authors already included the effect of nearby companion stars in their analysis of the *Kepler* light curves. The radii of Kepler-1 b, Kepler-5 b, Kepler-7 b, Kepler-13 b, Kepler-14 b, Kepler-64 b, and Kepler-432 b are already corrected for flux dilution by the nearby companion star. In most cases, this flux dilution is just a few tenths to a few percent, and therefore the change in the resulting planet radius is small (e.g., Esteves et al. 2015). The largest corrections to the transit depth (and thus planet radii) were applied for Kepler-13 b, Kepler-14 b, and Kepler-64 b (Buchhave et al. 2011; Szabó et al. 2011; Southworth 2012; Schwamb et al. 2013; Shporer et al. 2014; Esteves et al. 2015). We note that in general, even when the effect of the companion was included in the derivation of planet radii, usually only the case of planets orbiting their primary star was considered. The planet radius would change substantially if the planet orbited a fainter companion star.

The column "mass flag" in Table 1 identifies whether the mass of a planet was determined from RV measurements, TTVs, or a light-curve model (in some cases a combined model to multiple data sets; e.g., Schwamb et al. 2013). In cases where the planet mass was derived via RV measurements, it is clear that planets are orbiting the primary star (whose RV variations have been measured). Therefore, the companion stars in the Kepler-1, Kepler-5, Kepler-7, Kepler-10, Kepler-14, Kepler-21, Kepler-64, Kepler-74, Kepler-97, Kepler-106, Kepler-424, Kepler-432, and Kepler-448 systems cannot be the planet host stars. For Kepler-100, the situation is less clear, since planets c and d were not detected in the RV data and planet b only had a tentative detection (Marcy et al. 2014). So, we keep the possibility open that the Kepler-100 planets could orbit the companion star. Finally, based on centroid analysis of *Kepler* data, the primary stars in the Kepler-11 and Kepler-13 systems were determined to be the ones transited by the planets (Lissauer et al. 2011; Szabó et al. 2011).

For this work, we do not further consider those planets for which the companion star was excluded to be the planet host and its flux dilution has already been accounted for in the derived planet parameters. In addition, we also remove from our sample the Kepler-10, Kepler-11, Kepler-21, Kepler-106, and Kepler-424 systems, since the primary stars were found to be the planet hosts, and the flux dilution by the companion, while not corrected for, is very minute ($\lesssim$0.5%). The final sample we analyze in this work consists of 29 planets orbiting 15 stars (see Table 2). As with the planets' masses and radii, we adopted density measurements from the literature. In some cases, for a given planet only a mass (M) and radius (R) were published, but not the density; in those cases we carried out a simple calculation of the mean density ($\rho = M/(\frac{4}{3}\pi R^3)$, $\Delta\rho/\rho = \sqrt{(\Delta M/M)^2 + 9(\Delta R/R)^2}$). For published densities, we adopted the reported measurements and their uncertainties. When more than one density value was available for a given planet, we calculated a weighted average as we did for masses and radii. Planets with just an upper limit for their mass only have an upper limit for their density. Some planets have unrealistically high densities, both in published values and from our simple calculation. The likely reason is an overestimate of their masses; in several cases the masses were determined from TTVs, and a substantial underestimate of the orbital eccentricities leads to an overestimate of the planetary masses (there is a degeneracy between these two parameters; see Hadden & Lithwick 2014). In other cases the masses determined from radial velocities are very uncertain (e.g., Marcy et al. 2014), resulting in large uncertainties in the derived bulk densities.

Also listed in Table 1 are the planet radius correction factors (PRCF) from Furlan et al. (2017); since they only depend on stellar parameters, each planet in a multiplanet system has the same radius correction factor. Multiplying the planet radius by these factors yields the actual planet radius. There are two sets of factors: one assuming that planets orbit their primary star ("primary" factor hereafter), and one assuming that planets orbit the brightest companion star (under the assumption that it is bound to the primary star; "secondary" factor hereafter). The former is close to 1.0 in most cases; it is largest for Kepler-326 and Kepler-84, both of which have a nearby companion of almost equal brightness (at $0\farcs05$ with $\Delta K = 0.03$ for Kepler-326; at $0\farcs2$ with $\Delta m \sim 0.9$ at 0.55 μm for Kepler-84; Gilliland et al. 2015; Kraus et al. 2016). The radii of the planets in these two systems were derived from stellar radii and planet-to-star size ratios as reported in the literature, which do not seem to take into account the presence of the bright, nearby companions (Hadden & Lithwick 2014). No primary correction factor is listed for those planets for which the flux dilution by the companion has already been accounted for when the planet radius was derived.

For the secondary planet radius correction factors, there is a limit on how large they can be: the planet can only become as large as the companion star (thus obscuring 100% of the companion star during transit), which would also imply that it is likely not a planet, but a star. In these cases (Kepler-5, Kepler-106, Kepler-145, Kepler-424), the planet host stars do not have a secondary correction factor; moreover, the companion star is so faint that the primary correction factor is very small, less than 1%. The secondary factor is also not listed for those planets determined to orbit the primary star.

The planet radius correction factors can be converted to planet density correcting factors (PDCF), as $\mathrm{PDCF} = \mathrm{PRCF}^{-3}$. These factors are listed in Table 2, with one set assuming that planets orbit the primary star and one set assuming that planets orbit the brightest companion star. There is no secondary PDCF if planets were determined to orbit the primary star, which includes those systems in which companion stars could be excluded as being the planet hosts owing to the measured transit depth (see above). We used the calculated density correction factors to correct the planet bulk densities; these corrected densities are also listed in Table 2.

3. Results

3.1. Effect of Companions on Planet Bulk Density

Ciardi et al. (2015) estimated the effect of stellar companions on the derived planetary radii of all KOIs; they assumed that KOI host stars could be single or in binary or triple systems and that, in the case of multiple systems, the planets could orbit the primary star or one of the companion stars. They also assumed that the multiplicity of stars in the *Kepler* field is similar to that of stars in the solar neighborhood, as derived by Raghavan et al. (2010) and estimated by Horch et al. (2014). On average, they found that planet radii are underestimated by a factor of 1.49. In Furlan et al. (2017) we used the compiled measurements on 1903 KOI host stars with companions

Table 2
Bulk Densities, Planet Density Correction Factors, Orbital Periods, and Equilibrium Temperatures of *Kepler* Planets Studied in This Work

Planet Name (1)	ρ (g cm^{-3}) (2)	PDCF$_p$ (3)	PDCF$_s$ (4)	$\rho_{corr,p}$ (g cm^{-3}) (5)	$\rho_{corr,s}$ (g cm^{-3}) (6)	P (days) (7)	T_{eq} (K) (8)	References (9)
Kepler-27 b	1.151 ± 0.220	0.9597	0.0248	1.105	0.029	15.33	610	8, 12, 13
Kepler-27 c	0.317 ± 0.068	0.9597	0.0248	0.304	0.008	31.33	481	8, 12, 13
Kepler-53 b	24.811 ± 19.563	0.8540	0.1658	21.190	4.113	18.65	701	9, 12, 13
Kepler-53 c	6.465 ± 5.573	0.8540	0.1658	5.521	1.072	38.56	550	9, 12, 13
Kepler-74 b	0.584 ± 0.107	0.9101	…	0.531	…	7.34	1164	1, 3
Kepler-80 b	1.380 ± 0.205	0.9952	0.0066	1.373	0.009	7.05	546	4, 6
Kepler-80 c	1.220 ± 0.205	0.9952	0.0066	1.214	0.008	9.52	494	4, 6
Kepler-80 d	7.040 ± 1.060	0.9952	0.0066	7.006	0.046	3.07	720	4, 6
Kepler-80 e	3.750 ± 0.930	0.9952	0.0066	3.732	0.025	4.64	628	4, 6
Kepler-84 b	29.661 ± 24.648	0.5751	0.3745	17.058	11.109	8.73	985	10, 12, 13
Kepler-84 c	12.740 ± 12.313	0.5751	0.3745	7.327	4.772	12.88	865	10, 12, 13
Kepler-92 b	8.169 ± 1.914	0.9943	0.0343	8.123	0.280	13.75	975	11, 12, 13
Kepler-92 c	1.887 ± 0.620	0.9943	0.0343	1.876	0.065	26.72	781	11, 12, 13
Kepler-97 b	5.440 ± 3.480	0.9175	…	4.991	…	2.59	1328	12, 5
Kepler-100 b	14.250 ± 6.330	0.9755	0.0214	13.901	0.304	6.89	1155	5, 12
Kepler-100 c	<3.653	0.9755	0.0214	<3.564	<0.078	12.82	939	5, 12, 13
Kepler-100 d	<3.921	0.9755	0.0214	<3.825	<0.084	35.33	670	5, 12, 13
Kepler-104 b	3.540 ± 3.180	0.9961	0.0045	3.526	0.016	11.43	852	7, 12, 13
Kepler-145 b	11.038 ± 3.536	0.9997	…	11.035	…	22.95	873	11, 12, 13
Kepler-145 c	5.433 ± 1.222	0.9997	…	5.431	…	42.88	709	11, 12, 13
Kepler-203 c	…	0.9726	0.0272	…	…	5.37	1096	7, 12, 13
Kepler-203 d	…	0.9726	0.0272	…	…	11.33	855	7, 12, 13
Kepler-326 b	8.821 ± 17.488	0.3589	0.3486	3.166	3.075	2.25	1127	7, 12, 13
Kepler-326 c	4.418 ± 8.440	0.3589	0.3486	1.585	1.540	4.58	889	7, 12, 13
Kepler-326 d	2.745 ± 5.632	0.3589	0.3486	0.985	0.957	6.77	781	7, 12, 13
Kepler-333 b	36.962 ± 36.551	0.9729	0.0382	35.960	1.410	12.55	480	7, 12, 13
Kepler-396 b	9.718 ± 8.114	0.9970	0.0490	9.689	0.476	42.99	496	11, 12, 13
Kepler-396 c	0.656 ± 0.551	0.9970	0.0490	0.654	0.032	88.50	390	11, 12, 13
Kepler-448 b	<4.241	0.9382	…	<3.979	…	17.85	911	2, 12, 13

Note. Columns: (1) *Kepler* planet name; (2) planet density (either from the literature or derived in this work; see text for details); (3) and (4) planet density correction factors assuming that the planet orbits the primary or brightest secondary star, respectively; (5) and (6) planet densities corrected using the factors from columns (3) and (4), respectively; (7) planet's orbital period; (8) planet's equilibrium temperature; (9) references for the planet parameters listed.
References. (1) Bonomo et al. 2015; (2) Bourrier et al. 2015; (3) Hébrard et al. 2013; (4) MacDonald et al. 2016; (5) Marcy et al. 2014; (6) Muirhead et al. 2012; (7) Rowe et al. 2014; (8) Steffen et al. 2012; (9) Steffen et al. 2013; (10) Xie 2013; (11) Xie 2014; (12) Q1–Q17 DR25 KOI table; (13) this work.

detected within 4″; the median correction factors for planet radii assuming that planets orbit the primary or brightest companion star were 1.01 and 2.69, respectively. A weighted average of these correction factors yielded a median value of 1.38 if planets were assumed more likely to orbit the primary star; if assuming that planets are equally likely to orbit the primary and companion star, the median correction factor became 1.85. Hirsch et al. (2017) analyzed those companions from Furlan et al. (2017) found within 2″ of the primary star and with photometric measurements in at least two filters. They performed isochrone fits to estimate the stellar parameters of the companion stars and determined whether the detected companions are likely to be bound. Confirming the results of Horch et al. (2014), they found that most subarcsecond binaries are bound; about half of all companions at 2″ are bound. Using their results from the isochrone fits, Hirsch et al. (2017) derived an average planet radius correction factor of 1.65, assuming equal likelihood for the primary and secondary star to be hosting the planets.

The effect of changing the planet radius on its density is shown in Figure 1. A correction factor of 1.5 for the planet radius translates to a factor of 3.4 decrease in density. We note that while average correction factors for planet radii give an idea of the overall expected changes in planet radii, each individual planet will have an individual planet radius correction factor depending on its stellar system's configuration and which star the planet orbits. If a stellar system consists of two equal-brightness stars with the same stellar radii, the radius of the planet (derived assuming that the star is single) would

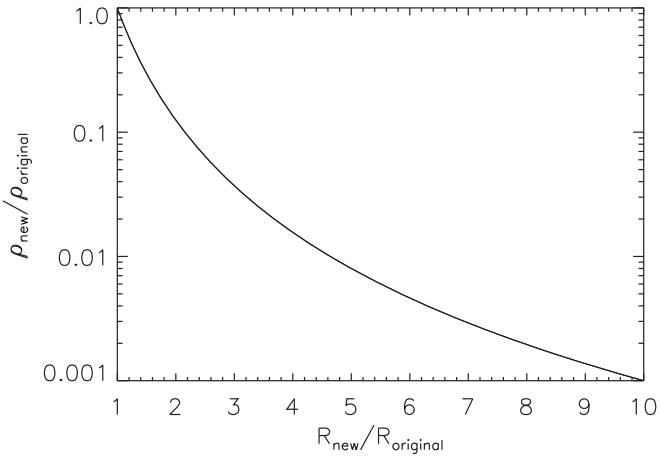

Figure 1. Fractional change of planet density vs. fractional change of planet radius. The subscript "new" identifies the new, corrected values, while the subscript "original" stands for the originally derived parameter value (for example, not taking into account the presence of a stellar companion).

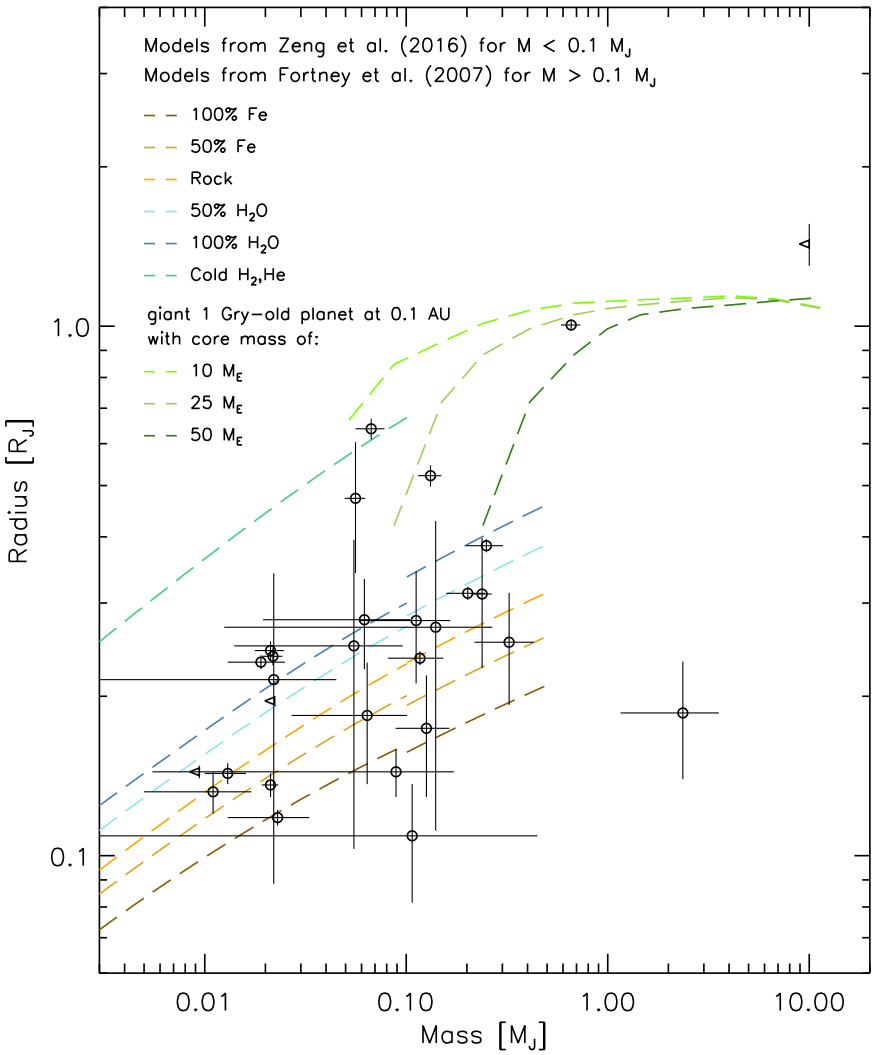

Figure 2. Radius vs. mass for confirmed *Kepler* planets whose host stars have stellar companions within 2″ and that still require corrections to their radii. The colored dashed lines represent planet models with different interior composition from Zeng et al. (2016) for $M < 0.1\ M_J$ and from Fortney et al. (2007) for $M > 0.1\ M_J$ (see label).

have to be revised upward by a factor of $\sqrt{2}$, resulting in a decrease in density by a factor of 2.8. If the primary star is brighter than the secondary star and the planet orbits the primary star, the correction factors for the radii are smaller, and thus the density decreases less. However, if a star has a relatively faint companion and the planet actually orbits this faint star, the radius of the planet can change by a factor of a few, and thus the density could decrease by 1–2 orders of magnitude.

3.2. Planet Density and Composition

In Figure 2 we plot the radii versus the masses of the *Kepler* planets from Table 2 (masses and radii are listed in Table 1). Also shown are model-derived mass–radius relations from Fortney et al. (2007) and Zeng et al. (2016); these models allow us to estimate the bulk composition of the planets in our sample and to evaluate how the densities change when the radii are corrected as a result of the presence of a stellar companion. For planets with masses in the ∼0.005–0.5 M_J range (which corresponds to 1.6–160 $M_\oplus$), the composition becomes more volatile-rich the larger the planet radius is; for example, with a mass of 0.01 M_J (=3.2 $M_\oplus$), a planet with a radius of 0.1 R_J (=1.1 $R_\oplus$) is expected to be composed of pure iron, while a radius larger by 30% and 70% implies a rocky and 100% water composition, respectively. To infer that this planet has an extensive hydrogen/helium atmosphere, its original radius of 0.1 R_J would have to be larger by a factor of 3.6, or equal to 4.0 $R_\oplus$. Planets with masses larger than about 0.1 M_J are expected to have inflated atmospheres if their radii are larger than ∼1.1 R_J (Lopez & Fortney 2014).

Figure 3 shows the same data points as Figure 2, but for each planet, two points are shown: one with the originally derived radius, and one with the radius corrected using the planet radius correction factors from Furlan et al. (2017). The left panel of the figure shows radii corrected with the primary factors, while the right panel displays radii corrected with the secondary factors. Since for these *Kepler* systems at least one companion star is present, even if planets orbit their primary star, a correction to the radius is needed. For those planets found to orbit the primary star (Kepler-74 b, Kepler-97 b, Kepler-145 b and c, and Kepler-448 b), no corrected radius is shown in the right panel of Figure 3. As mentioned in Section 2, even though there are RV measurements for Kepler-100, none of the planets in that system have a clear RV signal detection, and therefore we include them in both panels of Figure 3.

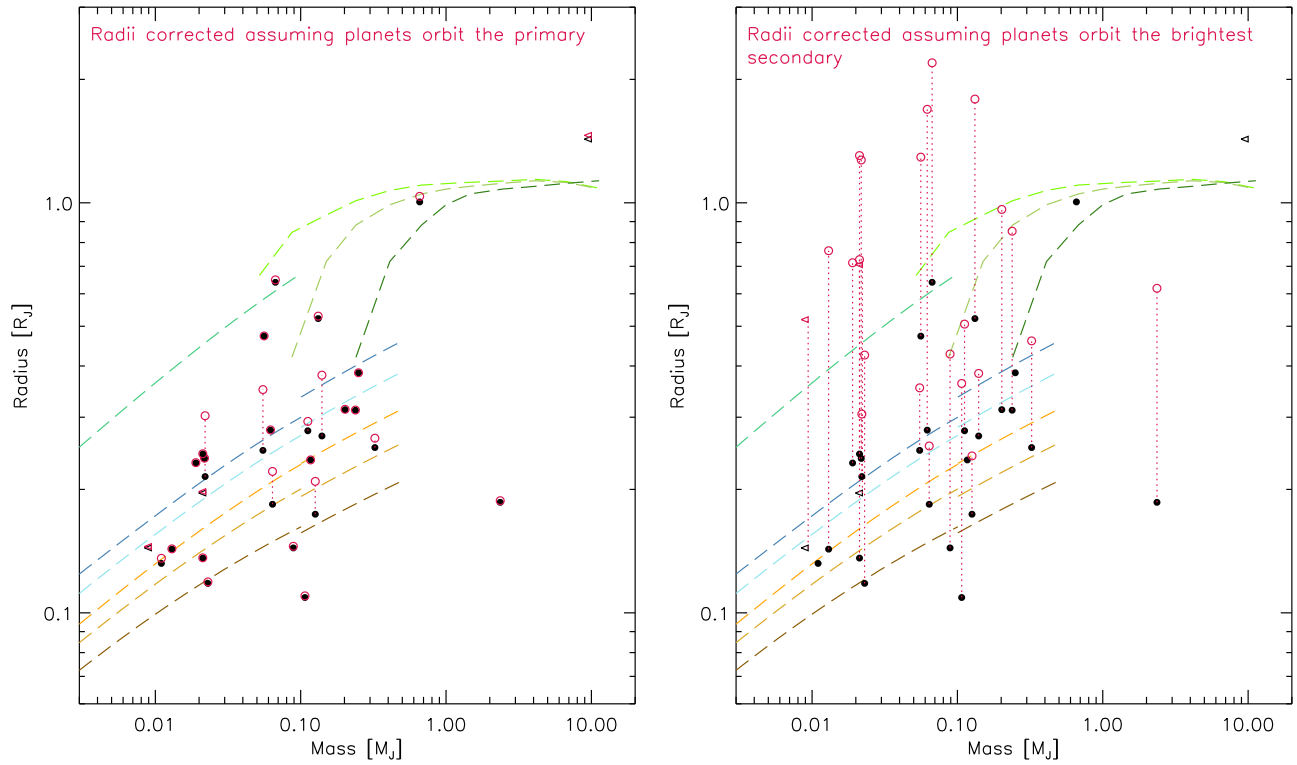

Figure 3. Similar to Figure 2; the black circles are measurements (for clarity, uncertainties are omitted), while the red circles result from correcting the radii assuming that the planets orbit the primary (left) or brightest companion star (right). The colored dashed lines have the same meaning as in Figure 2.

The planets shown in Figure 2 span a variety of bulk compositions, from iron-rich, volatile-free planets to more water-rich ones and planets with extensive atmospheres. Many planet masses (and, to a lesser extent, planet radii) are very uncertain, and so there is a range in possible planet composition for each planet. In Figure 4 we show histograms of the planet bulk densities, both for measured values and for values corrected owing to the presence of a companion star using the PDCFs from Table 2. The measured values range from 0.32 to over 20 g cm^{-3} (with the latter values very uncertain; see Table 2). Figure 5 displays the same bulk densities from Figure 4 as a function of orbital period, with symbol sizes scaled according to the planet's equilibrium temperature (which was adopted either as an average of published values, if available, or as the value from the Q1–Q17 Data Release 25 KOI table). It is expected that planets with short orbital periods are hot, and if they have extensive atmospheres, they may be inflated and thus have low densities. Indeed, about 40% of the planets in our sample with periods less than 10 days have equilibrium temperatures larger than 1000 K, while the planets with longer periods (>10 days) are all cooler than 1000 K.

When correcting the planet radii as a result of the flux dilution by the companion star, for 22 of the 29 planets in our sample the radii and thus also densities do not change noticeably if the planets are assumed to orbit their primary stars. Only three stars have companions that are bright enough to cause an obvious increase in the planet radius when accounting for its flux dilution. Kepler-326 and Kepler-84 are almost equal brightness binaries, and so the radii of Kepler-326 b, c, and d and those of Kepler-84 b and c increase by factors of 1.4 and 1.2, respectively. The most dramatic change occurs for the Kepler-326 planets, which, with their larger radii, are dominated by gaseous atmospheres (as opposed to a rock–

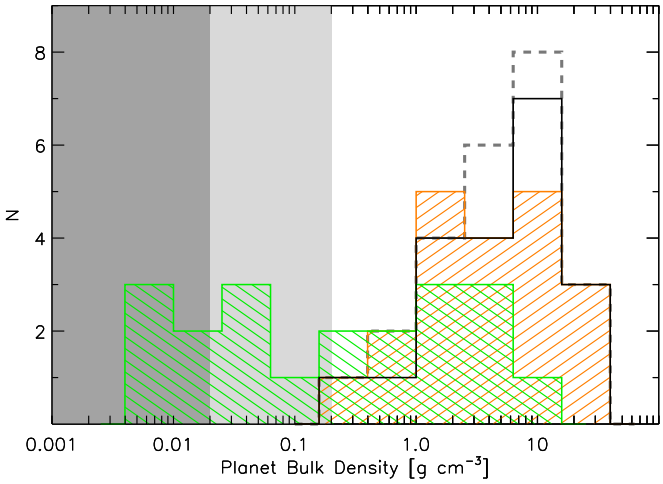

Figure 4. Histograms of the bulk densities of confirmed *Kepler* planets studied in this work (see Table 2). The gray dashed histogram shows all the measurements, excluding upper limits, while the black histogram shows only those planets for which both the primary and secondary density correction factors are defined (see text for details). The orange and green histograms show the densities after correcting the planet radii assuming that the planets orbit the primary or brightest companion star, respectively. The dark-gray area covers unphysically low densities, while the light-gray area covers densities of highly inflated planets.

volatiles mixture before radius correction). The two planets in the Kepler-53 system experience a 5% change in radius.

On the other hand, the changes can be substantial if planets are assumed to orbit the brightest companion star. In the latter case, most planets whose current density identifies them as rocky or water-rich would become gas giants. However, a large fraction of these planets would reach unrealistically low densities ($\lesssim$0.1 g cm^{-3}), which would require highly inflated

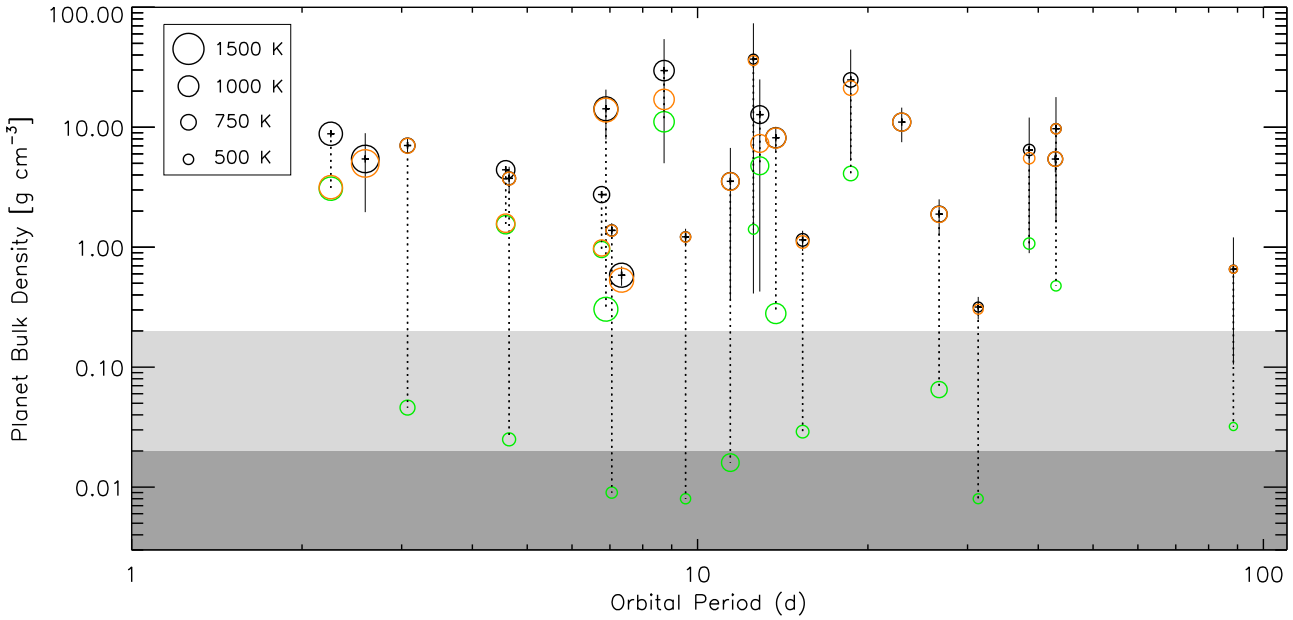

Figure 5. Bulk densities from Table 2 vs. the planet orbital period; the symbol sizes scale with the planet's equilibrium temperature as shown in the label. Black circles represent density measurements (and vertical solid lines their uncertainties), while the orange and green circles represent densities after correcting the planet radii assuming that the planets orbit the primary or brightest companion star, respectively. The gray areas have the same meaning as in Figure 4.

atmospheres (and high equilibrium temperatures) or unusually large ($\gtrsim$10%) mass fractions in an H/He envelope, both of which would not be stable, long-lived configurations (Lopez et al. 2012). Currently, the planets with the lowest densities (0.02–0.05 g cm^{-3}) are K2-97 b, Kepler-51 b, c, d, and HAT-P-67 b; K2-97 b and HAT-P-67 b orbit evolved stars and have highly inflated atmospheres (Grunblatt et al. 2016; Zhou et al. 2017), while the three planets in the Kepler-51 system have either massive H/He envelopes or underestimated masses, given that they were determined via TTVs (Masuda 2014). In Figures 4 and 5, the region of very low density planets ($\sim$0.02–0.2 g cm^{-3}) is indicated by a light-gray area, while densities lower than that (which are improbable, and thus likely unphysical) are encompassed by a dark-gray area. For those planets that end up in the low-density regime ($\lesssim$0.1 g cm^{-3}) after radius correction (8 of the 22 planets that could potentially orbit the companion star), the scenario of the planet orbiting the companion star can be excluded with a high degree of certainty. This includes Kepler-396 c; even though the density of Kepler-396 b would allow it to orbit the companion star, Kepler-396 c makes it unlikely for both planets to orbit the companion star. Overall, based on their masses, radii, and flux contamination by the companion star, we find that 15 planets in seven planetary systems could orbit either the primary or companion star (Kepler-53 b and c, Kepler-84 b and c, Kepler-92 b and c, Kepler-100 b, c, d, Kepler-203 c and d, Kepler-326 b, c, d, and Kepler-333 b).

4. Discussion

The density of a planet depends on both its mass and radius. While different methods exist to determine a planet's mass, some with fairly large uncertainties, the radii of transiting planets are usually known with smaller uncertainties than the mass (see Figure 2). However, the fact that many stars have nearby companion stars adds additional uncertainty to the radius determination. When companion stars have been detected in high-resolution imaging or spectroscopic follow-up observations, corrections to the planet radii due to flux dilution can be applied; they are usually relatively small if planets are assumed to orbit the primary star, but they can be large if planets orbit the companion star. Of particular concern are close binaries of about equal brightness (possibly $\sim$15% of stars); they require the largest correction in radius and thus density for planets orbiting the primary star (factors of $\sim$1.4 and 0.35, respectively). In our sample, Kepler-326 and Kepler-84 have such a bright, close companion and therefore experience the most significant change in the bulk composition of their planets.

In most cases, it is not known which star the planet orbits. Besides for very faint companion stars, which would result in planet radii larger than that of the star, RV measurements can allow us to exclude a companion star as the host, since the primary star's spectrum is the source of the RV information from which the planet mass is derived. However, for equal-mass (and thus equal-brightness) binaries, it could be difficult to determine which star is indeed the planet host; on the other hand, in this case the radius correction factors are similar for both stars in the system. In several multiplanet systems, planet masses have been determined from TTVs; in these cases, as opposed to RV detections, the star hosting the planets is not obvious. The only fairly certain assertion for systems with more than one planet is that all planets likely orbit the same star.

The planet bulk density can offer an important clue as to whether a planet can indeed orbit a companion star, given that in this case the density can decrease substantially (1–2 orders of magnitude). Low-density planets are known; many can be found in compact, multiplanet systems (e.g., Kepler-11, Lissauer et al. 2013; Kepler-51, Masuda 2014; Kepler-79, Jontof-Hutter et al. 2014). Among *Kepler* planets, Kepler-51 b, c, and d and Kepler-79 d have the lowest densities measured to date, ranging from 0.03 to 0.09 g cm^{-3} (Jontof-Hutter et al. 2014; Masuda 2014). Assuming that their masses are not underestimated, their low density implies that their

compositions are dominated, either by volume or by mass, by volatiles. If the incident flux is sufficiently high (a few hundred times the flux the Earth receives from the Sun), the atmosphere can be highly inflated, also resulting in a low density (Lopez & Fortney 2014).

The accretion of large amounts of volatiles onto a forming planet presents its own challenges; according to one model of giant planet formation, a core has to form first, and then a sufficient amount of gas has to be available to be accreted (see Helled et al. 2014). These conditions can be met beyond the snow line, with subsequent type I migration inward (e.g., Rogers et al. 2011). Planets with large H/He envelopes and relatively small cores (~10%–15% of volume) could be young or could have inflated radii as a result of strong stellar irradiation; these atmospheres could also suffer from photo-evaporation and thus become less massive over time (Rogers et al. 2011; Lopez et al. 2012). This atmospheric mass loss depends on the mass and size of the planet, as well as the stellar UV flux; it is expected to be strongest during the first few hundred megayears and could lead to the complete loss of an atmosphere in several gigayears for a planet with a mass of a few $M_{\oplus}$ (Rogers et al. 2011; Lopez et al. 2012). For planets with substantial atmospheres observed today, the atmospheric erosion would imply that the H/He envelopes were even more massive in the past, which compounds the challenge of forming substantial gaseous envelopes when the planet is still embedded in its protoplanetary disk. Overall, low-density planets seem to require special formation scenarios and conditions and are therefore expected to be rare. In turn, this might imply that few exoplanets orbit faint companion stars. Out of the 22 planets in our sample that could potentially orbit the companion star, we conclude that 8 can only orbit the primary star, since otherwise their densities would become lower than ~ 0.1 g cm^{-3}.

We note that our sample of 29 *Kepler* planets does not include any planets comparable to Earth in mass and size. Among the larger sample of *Kepler* planets with masses, radii, and companion stars within 2″, the planet with the smallest mass, Kepler-11 f, has a mass of 2.1 $M_{\oplus}$ and a radius of 2.5 $R_{\oplus}$, while the two planets with radii less than 1 $R_{\oplus}$, Kepler-106 b and d, only have upper limits in their masses (<5.4 and 7.9 $M_{\oplus}$, respectively). The effect of stellar companions on planet radii will be even more important for small, presumably rocky planets, since lower densities will imply more volatiles and possibly large atmospheres, conditions that are not suitable for life as we know on Earth. One problem with Earth-sized planets is that their masses are difficult to measure; in many cases, only radii will be measured directly. If mass–radius relationships are to be used to infer their masses (and densities), it is crucial to determine their radii accurately, which implies detecting any nearby companion star.

5. Conclusions

Given that about half the stars in the solar neighborhood are in multiple systems, and moreover about 15% of them have a close, roughly equal mass companion, it is important to determine whether a planet host star has a companion star. The presence of a companion will have an effect on the determination of the radius of a transiting planet owing to the dilution of the transit depth. We studied the effect of companion stars on the radii, and thus bulk densities, of those confirmed *Kepler* planets that have both masses and radii determined and whose stars have at least one stellar companion detected within 2″ that has not yet been taken into account when deriving the planets' radii and that could, in most cases, potentially be the planet host. Our sample contains 29 planets orbiting 15 stars. In a multiple-star system, it is often not known which star the planets orbit, but in either case the planetary radii will have to be revised upward. Even if the assumption is made that the planets are more likely to orbit the primary star, the planet radii would require an increase by as much as a factor of 1.4 and a corresponding decrease in bulk density by as much as a factor of 2.8. Such a decrease in density would change the composition of any iron-rich planet to that of a planet with at least some volatiles, and a rocky planet would become a planet dominated by volatiles.

Even more dramatic changes in the inferred planet bulk composition are expected if the planet orbits a fainter companion star; in this case several planets in our sample would be inferred to have extensive hydrogen/helium atmospheres (likely also highly inflated). This scenario is probably not very common, and it can be ruled out if the planet bulk density would become unrealistically low, but it has to be assessed on a case-by-case basis. Of particular interest are small, rocky planets; they are more affected by the presence of companion stars, since they could still be Earth-like (if orbiting the primary star) or dominated by volatiles (if orbiting a fainter companion star), and thus not be Earth-like at all. Since masses are very challenging to measure for small planets, it is critical to at least determine accurate radii for them in order to derive a good estimate of their mean density.

Of the 29 planets in our sample, seven experience notable increases in their radius once the effect of the companion star is folded in: Kepler-326 b, c, d, Kepler-84 b and c, and, to a lesser extent, Kepler-53 b and c. In particular, the Kepler-326 planets would change from a composition of rock and some volatiles to one dominated by a gaseous envelope. Five planets in our sample cannot orbit the companion star, since previous work determined that they orbit the primary star. Of the remaining planets with measured densities, eight would end up with unrealistically low densities if they orbited the companion star. Overall, we conclude that in seven planetary systems (with a total of 15 planets) the planets could orbit either the primary or the companion star (Kepler-53, Kepler-84, Kepler-92, Kepler-100, Kepler-203, Kepler-326, and Kepler-333).

The effect of a companion star on the bulk density of a planet underlines the importance of follow-up studies of host stars of planet candidates found with the transit method. High-resolution imaging and RV measurements will reveal companion stars in certain ranges of parameter space; in addition, in-depth statistical analysis using the observational results should allow us to infer which star the planet is most likely to orbit. Among the *Kepler* planet host stars, there are likely still many unidentified binary systems; for host stars that are closer (and brighter), as is the case for many *K2* and most *TESS* targets, fewer companions are missed by follow-up observations (e.g., Ciardi et al. 2015; Crossfield et al. 2015; Vanderburg et al. 2015; Howell et al. 2016). Thus, with appropriate follow-up work, the large expected planet yield of the *K2* and *TESS* missions, as well as other future transiting surveys, should result in more reliable planet radii and therefore more definitive identification of truly Earth-like planets in the solar neighborhood.

We thank our referee for useful suggestions that improved the presentation and clarity of the paper. Support for this work was provided by NASA through awards issued by JPL/Caltech. This research has made use of the NASA Exoplanet Archive and the Exoplanet Follow-up Observation Program website, which are operated by the California Institute of Technology, under contract with NASA under the Exoplanet Exploration Program. It has also made use of NASA's Astrophysics Data System Bibliographic Services.

Appendix A
Notes on Individual Planets

A.1. Planets Studied in This Work (Targets from Table 2)

Kepler-27 b and c.—The masses of Kepler-27 b and c were determined from TTVs by Hadden & Lithwick (2014); since these authors identified the planet pair as likely having high eccentricities, their masses are probably overestimated. From the measured masses and radii, we derive bulk densities of 1.15 and 0.32 g cm^{-3} for Kepler-27 b and c, respectively. Both planets seem to be gas giants, with a smaller core for Kepler-27 c than b. Steffen et al. (2012) raised the possibility that the planets could actually orbit the companion star $\sim 2''$ to the northeast ($\Delta K = 3.4$; Furlan et al. 2017). However, for this scenario we derived unrealistically low planet densities (<0.03 g cm^{-3}), which would decrease even more if the planet masses were actually lower.

Kepler-53 b and c.—Similar to the planets of Kepler-27, the masses of Kepler-53 b and c were determined from TTVs, and they are identified as high-eccentricity planets (Hadden & Lithwick 2014). We derive high bulk densities for both planets, but the uncertainties are large. Kepler-53 b is consistent with an iron-rich rocky composition, while Kepler-53 c is water-rich. If the dilution caused by the $0\farcs1$ companion ($\Delta m \sim 2.5$ at 0.55 μm; Gilliland et al. 2015) is taken into account, the planet densities decrease by about 15% if the planets are assumed to orbit the primary star, but by almost 85% if they are assumed to orbit the fainter star. In the latter case, both planets would be inferred to have substantial gaseous envelopes.

Kepler-74 b.—Kepler-74 b is a gas giant planet whose mass was determined from RV measurements (Hébrard et al. 2013; Bonomo et al. 2015). It has a relatively high equilibrium temperature of $\sim$1200 K. The star has a companion at a separation of $0\farcs3$, which is about 0.5 mag fainter in the optical (Ziegler et al. 2017). This companion was not taken into account when the planet radius was derived, and so, even though the planet is orbiting the primary (given its RV signal), its radius has to be revised by about 3%.

Kepler-80 b to e.—Kepler-80 is surrounded by five transiting planets (Xie 2013; Lissauer et al. 2014; Rowe et al. 2014; Morton et al. 2016), all of which have orbital periods less than 10 days. The densities of the four planets with mass and radius determinations imply a rocky composition for Kepler-80 d and e and substantial atmospheres for planets b and c (MacDonald et al. 2016). We can exclude the scenario that the planets orbit the $1\farcs7$-companion star of Kepler-80 ($\Delta K = 5.2$; Kraus et al. 2016) since the densities of at least some of the planets in each system would become unrealistically low.

Kepler-84 b and c.—Kepler-84 is among those systems for which the planet radii, and thus planet densities, change substantially even if the planets orbit their primary star, since the companion star at $0\farcs2$ is only somewhat fainter than the primary ($\Delta m \sim 0.9$ at 0.55 μm; Gilliland et al. 2015). Its primary and secondary planet radius correction factors are 1.202 and 1.387, respectively (Furlan et al. 2017). It is surrounded by five planets, of which only two have measured masses from TTVs (Hadden & Lithwick 2014). The composition of Kepler-84 b and c implies iron-rich solids; with the larger planet radii, they would still be rocky planets, but in the case of Kepler-84 c (whose mass is about a factor of two lower than that of Kepler-84 b), the new density suggests the additional presence of some water or other volatiles.

Kepler-92 b and c.—The masses of Kepler-92 b and c were determined from TTVs (Xie 2014). With a mass of 0.2 M_J, Kepler-92 b is 10 times as massive as Kepler-92 c. Their radii both lie in the Neptune-size regime. From their position in the mass–radius diagram, their composition is likely rich in volatiles. If they orbited the faint companion star instead of the primary (which is about 4.2 mag fainter in the K band and at a projected separation of $1\farcs5$; Kraus et al. 2016; Furlan et al. 2017), Kepler-92 c would be among the lowest-density planets, while Kepler-92 b would be a typical gas giant.

Kepler-97 b.—Kepler-97 is orbited by two planets, but only one (Kepler-97 b) has both mass and radius determined; the other one, Kepler-97 c, was detected in RV data as a linear trend, so only a lower limit of $\sim$1 M_J for its mass could be derived (Marcy et al. 2014). Kepler-97 has a fainter companion at a separation of $0\farcs4$ ($\Delta K = 3$; Furlan et al. 2017); Marcy et al. (2014) suggested that it could be the cause for the linear trend in the RVs (and thus Kepler-97 c would not exist). They also concluded that Kepler-97 b most likely orbits the primary star based on the lack of centroid shift when comparing the in- and out-of-transit photocenters. However, Marcy et al. (2014) did not correct the planet radius given the flux dilution caused by the companion star (since it is a relatively small correction of 3%; Furlan et al. 2017).

Kepler-100 b, c, d.—There are three planets in the Kepler-100 system, but only one, Kepler-100 b, has a measured mass from RV data, albeit with just a tentative RV signal detection (Marcy et al. 2014). Given the tentative RV signal of just one planet, we did not exclude the fainter companion star (at a projected separation of $1\farcs8$, with $\Delta i = 4.2$; Lillo-Box et al. 2014; Furlan et al. 2017) from being the planet host. The density of Kepler-100 b implies an iron-rich composition, but since its mass is fairly uncertain, it could be more rich in volatiles. The upper limits in mass for Kepler-100 c and d suggest that they are volatile-rich planets. If the planets orbited the companion star, they would be low-density giant planets, with Kepler-100 c and d among the lowest-density planets known.

Kepler-104 b.—The Kepler-104 multiplanet system contains three planets of similar size (Rowe et al. 2014), but only Kepler-104 b has a mass determined from TTVs (Hadden & Lithwick 2014). Since it is flagged as a high-eccentricity planet by Hadden & Lithwick (2014), its mass could be overestimated. Its measured mass implies a composition dominated by volatiles. If Kepler-104 b orbited the faint companion star at $1\farcs9$ from the primary ($\Delta i = 6.1$; Lillo-Box et al. 2014), its density would become unrealistically low.

Kepler-145 b and c.—The masses of Kepler-145 b and c were determined from TTVs (Xie 2014). Kepler-145 c is both larger and more massive than Kepler-145 b; its composition is likely dominated by volatiles, while Kepler-145 b is mostly rocky. The very faint companion star at a projected separation

of 1.″5 ($\Delta K = 8.5$; Kraus et al. 2016) causes a negligible flux dilution (primary planet radius correction of 1.0001; Furlan et al. 2017); we conclude that the companion cannot be the planet host since the planets would become bigger than the star.

Kepler-203 c and d.—Kepler-203 is orbited by three planets (Rowe et al. 2014), but only the two outermost planets, Kepler-203 c and d, have masses determined from TTVs (Hadden & Lithwick 2014). The location of Kepler-203 c and d in the mass–radius diagram implies a density higher than pure iron. However, they were flagged as high-eccentricity planets, which suggests that their masses are overestimated (Hadden & Lithwick 2014). Masses lower by at least an order of magnitude would make these planets consistent with a rocky or water-rich composition. On the other hand, if Kepler-203 c and d transited the companion star (located at 1.″9, with $\Delta i = 4.1$; Lillo-Box et al. 2014; Furlan et al. 2017) instead of the primary, their radii would be larger by about a factor of three, and thus, even if their masses did not change, their density would be low enough to be consistent with that of a gas giant planet.

Kepler-326 b, c, d.—Similar to Kepler-84, the planets of Kepler-326 require substantial revisions to their radii and densities even if they orbit the primary star. The primary and secondary planet radius correction factors are 1.407 and 1.421, respectively (resulting from an almost equal brightness binary; the two stars are just 0.″05 apart; Kraus et al. 2016). Kepler-326 has three planets, all of which have measured masses from TTVs (Hadden & Lithwick 2014). After correcting for the flux dilution by the companion, the increased planetary radii imply substantial atmospheres as opposed to water-dominated (Kepler-326 c and d) or water–rock (Kepler-326 b) composition.

Kepler-333 b.—The mass of Kepler-333 b was determined from TTVs (Hadden & Lithwick 2014). There is another planet in the system, Kepler-333 c, without a mass determination, but with a somewhat smaller radius (Rowe et al. 2014). The density of Kepler-333 b implies a density higher than pure iron. If its mass were lower by at least a factor of 10, its composition would be consistent with that of rock or a rock–water mixture. Similar to the Kepler-203 system, if Kepler-333 b orbited the companion star (separated by 1.″3 from the primary, with $\Delta i = 4.1$; Ziegler et al. 2017), its mass and radius would be consistent with that of a gas giant planet.

Kepler-396 b and c.—The masses and radii of Kepler-396 b and c imply a volatile-rich composition for planet b, while planet c, which is larger and less massive, is similar to a gas giant. Since masses were determined from TTVs (Xie 2014), they may be overestimated. If the planets orbited the faint companion, separated by 0.″6 from the primary and about 6 mag fainter in the optical (Furlan et al. 2017), Kepler-396 b would become an envelope-dominated planet, while the density of Kepler-396 c would become unrealistically low. Therefore, it is likely that both planets orbit the primary star.

Kepler-448 b.—Kepler-448 b is a 1.4 R_J planet with only an upper limit of 10 M_J for its mass derived from RV measurements (Bourrier et al. 2015). Its large radius (1.4 R_J) implies a highly inflated atmosphere (irrespective of the mass of the planet), but, as opposed to Kepler-13 b, which has a similarly large radius, it does not have a particularly high equilibrium temperature. From the analysis of time-series spectra, Bourrier et al. (2015) found that the transit is associated with Kepler-448; even though they were not aware of any companion stars, we conclude that the companion star located at 0.″6 from the primary (with $\Delta K = 3.8$; Kraus et al. 2016) is unlikely to be the planet host. However, even if Kepler-448 b orbits the primary star, its radius has to be corrected owing to the flux dilution by the companion (a small increase of 2%; Furlan et al. 2017).

A.2. Remaining Targets from Table 1

Kepler-1 b.—Kepler-1 b, also known as TrES-2 b, was discovered by O'Donovan et al. (2006); since its discovery, many authors have measured its properties from the *Kepler* light curve and ancillary data (see Table 1). Several authors did correct for the flux dilution by the faint companion (at 1.″1 with $\Delta i \sim 4$; Law et al. 2014), but the correction to the planet radius is just ∼1% (Furlan et al. 2017). With a mass of 1.22 M_J, a radius of 1.21 R_J, and an equilibrium temperature of 1470 K (Esteves et al. 2015), Kepler-1 b is a hot Jupiter with a somewhat inflated radius. Given that its mass was determined from RV measurements (e.g., O'Donovan et al. 2006), we can exclude the companion star as being the host.

Kepler-5 b.—Kepler-5 b is about one-third larger than Jupiter and twice as massive. Its large radius, as well as its equilibrium temperature of 1750 K (Esteves et al. 2015), suggests that its atmosphere is inflated. Similar to Kepler-1 b, the mass of Kepler-5 b was determined from RV measurements (Koch et al. 2010), and the companion at 0.″9 is about 5 mag fainter than the primary in the J band (Furlan et al. 2017), so the companion star cannot be the planet host. Also, the (very small) flux dilution by the companion was taken into account when the planet parameters for Kepler-5 b were derived (Koch et al. 2010; Southworth 2011).

Kepler-7 b.—Kepler-7 b stands out as a planet with a very large radius (1.6 R_J), small mass (0.4 M_J), and thus extremely low density (0.14 g cm^{-3}; Esteves et al. 2015). Its atmosphere is likely highly inflated, a result of its close orbit around a slightly evolved star (Latham et al. 2010), resulting in a high equilibrium temperature of 1630 K (Esteves et al. 2015). The host star has a faint companion ($\Delta i = 4.6$) at a projected separation of 1.″9 (Latham et al. 2010; Adams et al. 2012; Law et al. 2014), which was taken into account when the planet parameters for Kepler-7 b were derived (Latham et al. 2010; Southworth 2010, 2011). Moreover, the companion was excluded from being the star with the transit owing to the small observed centroid shifts, in addition to the primary's measured RV shifts (Latham et al. 2010).

Kepler-10 b and c.—There are two planets in the the Kepler-10 system: both Kepler-10 b and c have a relatively high density of ∼7–8 g cm^{-3} (Dumusque et al. 2014; Esteves et al. 2015), but the former has a mass of about 4 $M_\oplus$ and a radius of 1.5 $R_\oplus$, while the latter is more massive and larger with 17.2 $M_\oplus$ and 2.4 $R_\oplus$ (Lissauer et al. 2011, 2013; Hadden & Lithwick 2014). The densities of both planets imply a rocky composition, with Kepler-10 b containing some iron and Kepler-10 c likely some water (Dumusque et al. 2014). The absence of an atmosphere and the high equilibrium temperature of Kepler-10 b (2130 K; Esteves et al. 2015) suggest that it may be the remnant core of a gas-rich planet whose atmosphere was lost owing to photoevaporation (Lopez & Fortney 2014). Given that the masses of the planets in the Kepler-10 system were derived from RV measurements, the 2″ companion star ($\Delta K = 6.8$; Kraus et al. 2016) cannot be the planet host. Its flux dilution has not been taken into account previously, but the correction factor for the planet radius is negligible at 1.0005 (Furlan et al. 2017).

Kepler-11 b to g.—The Kepler-11 system consists of six transiting planets. The masses of five planets (b through f) were determined from TTVs (planet g has only an upper limit in mass), and their densities imply large volume fractions of volatiles, like H_2O, CH_4, H_2, and He (Lissauer et al. 2011, 2013; Hadden & Lithwick 2014). The planets around Kepler-11 form a tight planetary system; they all orbit within 0.5 au from their star (Lissauer et al. 2013). A faint companion star ($\Delta K = 4.6$) lies at a separation of 1.″3 (Wang et al. 2015a; Kraus et al. 2016); its flux dilution has not been considered previously, but it is very small, causing a radius change of less than 0.5% (Furlan et al. 2017). Based on centroid analysis of *Kepler* data, Lissauer et al. (2011) concluded that the companion star cannot be the planet host.

Kepler-13 b.—Kepler-13 b has a very large mass (9.0 M_J) and also large radius (1.5 R_J), implying a substantial atmosphere (Shporer et al. 2014; Esteves et al. 2015). It also has a high equilibrium temperature of 2550 K (Esteves et al. 2015). In fact, it was found to likely orbit the brighter star of a 1″ binary, of which both components are rapidly rotating A-type stars (Szabó et al. 2011). With a period of just 1.7 days, it is a hot Jupiter with a highly inflated atmosphere (e.g., Shporer et al. 2014). The transit depth dilution by the companion was taken into account when the radius of Kepler-13 b was derived (Shporer et al. 2014; Esteves et al. 2015).

Kepler-14 b.—Similar to Kepler-13 b, Kepler-14 b has a very large mass (8.1 M_J; Buchhave et al. 2011; Southworth 2012). It is a bit smaller than Kepler-13 b, which implies a higher bulk density. The almost equal brightness companion star at a separation of just 0.″3 was taken into account in the light-curve fit and in the derivation of the RVs (Buchhave et al. 2011). Moreover, from centroid analysis of *Kepler* data Buchhave et al. (2011) concluded that the primary star is the planet host.

Kepler-21 b.—The mass and radius of Kepler-21 b, 5.1 $M_\oplus$ and 1.64 $R_\oplus$, respectively, indicate that it is likely a rocky planet (López-Morales et al. 2016). Given its high equilibrium temperature of ∼2000 K (it is in a 2.8-day orbit around a star with $T_{\rm eff} = 6300$ K), López-Morales et al. (2016) suggested that the planet is surrounded by a thick layer of molten rock; it could be the leftover core of a giant planet. The mass of Kepler-21 b has been determined from RV measurements, so we can exclude the faint companion ($\Delta K = 4$; Kraus et al. 2016; Furlan et al. 2017) at a projected separation of 0.″8 as the planet host star. López-Morales et al. (2016) were not aware of this companion, so its flux dilution has not been accounted for, but it is very small (Furlan et al. 2017).

Kepler-64 b.—Kepler-64 b is a circumbinary planet; its host star actually forms a quadruple stellar system, with an eclipsing binary and wider binary at a separation of ∼0.″7 (Schwamb et al. 2013). In addition, there is a faint star at a projected separation of 3″. The flux dilution by these companions (about 13%) was taken into account by Schwamb et al. (2013) when deriving the transit depth and thus planet radius of Kepler-64 b. They also derived an upper limit for the mass, which, combined with the radius measurement, places this planet in the gas giant regime. Based on the RV measurements and models of Schwamb et al. (2013), it is clear that the eclipsing binary star is the host.

Kepler-106 b to e.—Kepler-106 has a total of four planets, with RV yielding mass measurements for planets c and e and upper limits for the mass of planets b and d (Marcy et al. 2014). Kepler-106 b and d are probably consistent with an iron-rich or rocky composition. On the other hand, Kepler-106 c and e are volatile-rich. Given the very faint companion star at 1.″7 from the primary ($\Delta K = 8.5$; Kraus et al. 2016), the transit dilution is minimal (and so it does not matter that it was not taken into account by Marcy et al. 2014); moreover, the companion star cannot be the planet host, since, in addition to the RV detections of planets c and e in the spectrum of the primary, in this case the planets would become bigger than the star.

Kepler-424 b.—There are two planets in the Kepler-424 system: Kepler-424 b is a hot Jupiter that transits the star during its 3.3-day orbit, and Kepler-424 c is a ∼7 M_J planet on a 223-day orbit that was detected in RV data and does not transit (Endl et al. 2014). Thus, only Kepler-424 b has both mass and radius determined. The close companion star (at 0.″07) is faint ($\Delta K = 3.7$; Kraus et al. 2016) and thus would cause a very minor correction to the planet radius and density. Therefore, similar to some of the other planets presented here, it does not really matter that it was not taken into account previously. It cannot be the planet host, since both planets were detected in the RV data of the primary.

Kepler-432 b.—Similar to the Kepler-424 system, Kepler-432 is orbited by a transiting planet (Kepler-432 b) and another planet (Kepler-432 c), detected in RV data, that does not transit (Quinn et al. 2015). However, the host star is a red giant star, and the orbit of Kepler-432 b is very eccentric (Ciceri et al. 2015; Quinn et al. 2015). Kepler-432 b is also fairly massive (∼5.2 M_J), and its radius of 1.13 R_J places it at the lower end of the inflated gas giant regime. The flux dilution by the 0.″9 companion ($\Delta K = 5.1$; Kraus et al. 2016; Furlan et al. 2017) was taken into account when analyzing the light curve of Kepler-432 b (Ciceri et al. 2015), but the effect is very small. Given the RV data, the companion can be excluded as the planet host.

References

Adams, E. R., Ciardi, D. R., Dupree, A. K., et al. 2012, AJ, 144, 42
Barclay, T., Huber, D., Rowe, J. F., et al. 2012, ApJ, 761, 53
Barclay, T., Quintana, E. V., Adams, F. C., et al. 2015, ApJ, 809, 7
Barnes, J. R., Jenkins, J. S., Jones, H. R. A., et al. 2014, MNRAS, 439, 3094
Batalha, N. M., Borucki, W. J., Bryson, S. T., et al. 2011, ApJ, 729, 27
Batalha, N. M., Rowe, J. F., Bryson, S. T., et al. 2013, ApJS, 204, 24
Bonomo, A. S., Sozzetti, A., Santerne, A., et al. 2015, A&A, 575, A85
Borucki, W. J., Koch, D., Basri, G., et al. 2010, Sci, 327, 977
Borucki, W. J., Koch, D. G., Basri, G., et al. 2011, ApJ, 736, 19
Bourrier, V., Lecavelier des Etangs, A., Hébrard, G., et al. 2015, A&A, 579, A55
Bryson, S. T., Jenkins, J. M., Gilliland, R. L., et al. 2013, PASP, 125, 889
Buchhave, L. A., Latham, D. W., Carter, J. A., et al. 2011, ApJS, 197, 3
Christiansen, J. L., Ballard, S., Charbonneau, D., et al. 2011, ApJ, 726, 94
Ciardi, D. R., Beichman, C. A., Horch, E. P., & Howell, S. B. 2015, ApJ, 805, 16
Ciceri, S., Lillo-Box, J., Southworth, J., et al. 2015, A&A, 573, L5
Crossfield, I. J. M., Petigura, E., Schlieder, J. E., et al. 2015, ApJ, 804, 10
Daemgen, S., Hormuth, F., Brandner, W., et al. 2009, A&A, 498, 567
Doyle, L. R., Carter, J. A., Fabrycky, D. C., et al. 2011, Sci, 333, 1602
Dumusque, X., Bonomo, A. S., Haywood, R. D., et al. 2014, ApJ, 789, 154
Duquennoy, A., & Mayor, M. 1991, A&A, 248, 485
Endl, M., Caldwell, D. A., Barclay, T., et al. 2014, ApJ, 795, 151
Esteves, L. J., De Mooij, E. J. W., & Jayawardhana, R. 2015, ApJ, 804, 150
Fogtmann-Schulz, A., Hinrup, B., Van Eylen, V., et al. 2014, ApJ, 781, 67
Fortney, J. J., Marley, M. S., & Barnes, J. W. 2007, ApJ, 659, 1661
Fressin, F., Torres, G., Désert, J.-M., et al. 2011, ApJS, 197, 5
Furlan, E., Ciardi, D. R., Everett, M. E., et al. 2017, AJ, 153, 71

Gilliland, R. L., Cartier, K. M. S., Adams, E. R., et al. 2015, AJ, 149, 24
Gillon, M., Jehin, E., Lederer, S. M., et al. 2016, Natur, 533, 221
Gillon, M., Triaud, A. H. M., Demory, B.-O., et al. 2017, Natur, 542, 456
Grunblatt, S. K., Huber, D., Gaidos, E. J., et al. 2016, AJ, 152, 185
Hadden, S., & Lithwick, Y. 2014, ApJ, 787, 80
Hébrard, G., Almenara, J.-M., Santerne, A., et al. 2013, A&A, 554, A114
Helled, R., Bodenheimer, P., Podolak, M., et al. 2014, in Protostars and Planets VI, ed. H. Beuther et al. (Tucson, AZ: Univ. Arizona Press), 643
Hirsch, L. A., Ciardi, D. R., Howard, A. W., et al. 2017, AJ, 153, 117
Holman, M. J., Winn, J. N., Latham, D. W., et al. 2007, ApJ, 664, 1185
Horch, E. P., Howell, S. B., Everett, M. E., & Ciardi, D. R. 2014, ApJ, 795, 60
Howell, S. B., Everett, M. E., Horch, E. P., et al. 2016, ApJL, 829, L2
Howell, S. B., Rowe, J. F., Bryson, S. T., et al. 2012, ApJ, 746, 123
Howell, S. B., Sobeck, C., Haas, M., et al. 2014, PASP, 126, 398
Jontof-Hutter, D., Lissauer, J. J., Rowe, J. F., & Fabrycky, D. C. 2014, ApJ, 785, 15
Kipping, D., & Bakos, G. 2011, ApJ, 733, 36
Koch, D. G., Borucki, W. J., Rowe, J. F., et al. 2010, ApJL, 713, L131
Kolbl, R., Marcy, G. W., Isaacson, H., & Howard, A. W. 2015, AJ, 149, 18
Kostov, V. B., Orosz, J. A., Welsh, W. F., et al. 2016, ApJ, 827, 86
Kraus, A. L., Ireland, M. J., Huber, D., et al. 2016, AJ, 152, 8
Latham, D. W., Borucki, W. J., Koch, D. G., et al. 2010, ApJL, 713, L140
Law, N. M., Morton, T., Baranec, C., et al. 2014, ApJ, 791, 35
Lillo-Box, J., Barrado, D., & Bouy, H. 2014, A&A, 566, A103
Lissauer, J. J., Fabrycky, D. C., Ford, E. B., et al. 2011, Natur, 470, 53
Lissauer, J. J., Jontof-Hutter, D., Rowe, J. F., et al. 2013, ApJ, 770, 131
Lissauer, J. J., Marcy, G. W., Bryson, S. T., et al. 2014, ApJ, 784, 44
Lopez, E. D., & Fortney, J. J. 2014, ApJ, 792, 1
Lopez, E. D., Fortney, J. J., & Miller, N. 2012, ApJ, 761, 59
López-Morales, M., Haywood, R. D., Coughlin, J. L., et al. 2016, AJ, 152, 204
MacDonald, M. G., Ragozzine, D., Fabrycky, D. C., et al. 2016, AJ, 152, 105
Marcy, G. W., Isaacson, H., Howard, A. W., et al. 2014, ApJS, 210, 20
Masuda, K. 2014, ApJ, 783, 53
Mathur, S., Huber, D., Batalha, N. M., et al. 2017, ApJS, 229, 30
Morton, T. D., Bryson, S. T., Coughlin, J. L., et al. 2016, ApJ, 822, 86
Muirhead, P. S., Hamren, K., Schlawin, E., et al. 2012, ApJL, 750, L37
O'Donovan, F. T., Charbonneau, D., Mandushev, G., et al. 2006, ApJL, 651, L61
Orosz, J. A., Welsh, W. F., Carter, J. A., et al. 2012, Sci, 337, 1511
Quinn, S. N., White, T. R., Latham, D. W., et al. 2015, ApJ, 803, 49
Raetz, S., Maciejewski, G., Ginski, C., et al. 2014, MNRAS, 444, 1351
Raghavan, D., McAllister, H. A., Henry, T. J., et al. 2010, ApJS, 190, 1
Rogers, L. A. 2015, ApJ, 801, 41
Rogers, L. A., Bodenheimer, P., Lissauer, J. J., & Seager, S. 2011, ApJ, 738, 59
Rowe, J. F., Bryson, S. T., Marcy, G. W., et al. 2014, ApJ, 784, 45
Schwamb, M. E., Orosz, J. A., Carter, J. A., et al. 2013, ApJ, 768, 127
Seager, S., Kuchner, M., Hier-Majumder, C. A., & Militzer, B. 2007, ApJ, 669, 1279
Shporer, A., O'Rourke, J. G., Knutson, H. A., et al. 2014, ApJ, 788, 92
Southworth, J. 2010, MNRAS, 408, 1689
Southworth, J. 2011, MNRAS, 417, 2166
Southworth, J. 2012, MNRAS, 426, 1291
Sozzetti, A., Guillermo, T., Charbonneau, D., et al. 2007, ApJ, 664, 1190
Steffen, J. H., Fabrycky, D. C., Agol, E., et al. 2013, MNRAS, 428, 1077
Steffen, J. H., Fabrycky, D. C., Ford, E. B., et al. 2012, MNRAS, 421, 2342
Szabó, Gy. M., Sazbó, R., Benkő, J. M., et al. 2011, ApJL, 736, L4
Teske, J. K., Everett, M. E., Hirsch, L., et al. 2015, AJ, 150, 144
Torres, G., Winn, J. N., & Holman, M. J. 2008, ApJ, 677, 1324
Turner, J. D., Pearson, K. A., Biddle, L. I., et al. 2016, MNRAS, 459, 789
Vanderburg, A., Montet, B. T., Johnson, J. A., et al. 2015, ApJ, 800, 59
Wang, J., Fischer, D. A., Horch, E. P., & Xie, J.-W. 2015a, ApJ, 806, 248
Wang, J., Fischer, D. A., Xie, J.-W., & Card, D. R. 2014a, ApJ, 791, 111
Wang, J., Fischer, D. A., Xie, J.-W., & Ciardi, D. R. 2015b, ApJ, 813, 130
Wang, J., Xie, J.-W., Barclay, T., & Fischer, D. A. 2014b, ApJ, 783, 4
Welsh, W. F., Orosz, J. A., Carter, J. A., et al. 2012, Natur, 481, 475
Xie, J.-W. 2013, ApJS, 208, 22
Xie, J.-W. 2014, ApJS, 210, 25
Zeng, L., Sasselov, D. D., & Jacobsen, S. B. 2016, ApJ, 819, 127
Zhou, G., Bakos, G. Á., Hartman, J. D., et al. 2017, AJ, 153, 211
Ziegler, C., Law, N. M., Morton, T., et al. 2017, AJ, 153, 66